Journal of Bioenergetics and Biomembranes, Vol. 36, No. 5, October 2004 (© 2004)

Mitochondrial Respiratory Chain Complex Patterns from *Acanthamoeba castellanii* and *Lycopersicon esculentum*: Comparative Analysis by BN-PAGE and Evidence of Protein–Protein Interaction between Alternative Oxidase and Complex III

Rachel Navet,[1] Wieslawa Jarmuszkiewicz,[2] Pierre Douette,[1] Claudine M. Sluse-Goffart,[1] and Francis E. Sluse[1,3]

Received

We have previously shown that a kinetic interplay exists between the cytochrome pathway and the alternative oxidase in mitochondria from amoeba *Acanthamoeba castellanii*. Native interaction analyses using blue native gel electrophoresis coupled to denaturating electrophoresis and immunodetection have indicated associations between alternative oxidase and oxidative phosphorylation complexes in both amoeba and tomato mitochondria. These associations are dependent on the expression level of alternative oxidase according to the physiological state in both organisms. Alternative oxidase associates broadly with large complexes of the respiratory chain when it is expressed in large amount, i.e., in ripe tomato and exponentially growing amoeba. On the contrary, alternative oxidase interacts specifically with complex III even if expression of the oxidase is low, i.e., in green tomato and stationary phase amoeba. This specific interaction represents a higher level of regulation driven by protein–protein interactions leading to a direct kinetic interplay between the cytochrome pathway and alternative oxidase in both plant and amoeba mitochondria.

KEY WORDS: Mitochondria; blue native electrophoresis; alternative oxidase; respiratory chain complexes; protein–protein interactions; *Acanthamoeba castellanii*; *Lycopersicon esculentum*.

INTRODUCTION

The mitochondrial respiratory chains of *Acanthamoeba castellanii*, a free-living soil amoeba, and of tomato *Lycopersicon esculentum*, a higher plant, share several common constitutive and functional features. Indeed, two pathways compete to oxidize ubiquinol, i.e., the cyanide-sensitive proton pumping cytochrome pathway (energy conserving) and the cyanide-resistant benzohydroxamate (BHAM)-sensitive alternative oxidase (AOX) that reduces oxygen without proton pumping (energy dissipating). Protozoan and plant respiratory chains are also able to oxidize external nicotinamide adenine dinucleotide (NADH) by rotenone-insensitive external NADH dehydrogenase without proton pumping and possess a non-electrogenic rotenone-insensitive internal NADH dehydrogenase that compete with complex I for matricial NADH.

[1] Laboratory of Bioenergetics, Department of Life Sciences, Institute of Chemistry B6c, University of Liège, Sart Tilman, Liège, Belgium.

[2] Laboratory of Bioenergetics, Institute of Molecular Biology and Biotechnology, Adam Mickiewicz University, Fredry 10, Poznan, Poland.

[3] To whom correspondence should be addressed at Laboratory of Bioenergetics, Department of Life Sciences, Institute of Chemistry B6c, University of Liège, Sart Tilman, Liège, Belgium; e-mail: F.Sluse@ulg.ac.be.

Key to abbreviations: AOX, alternative oxidase; BHAM, benzohydroxamic acid; GMP, guanosine monophosphate; Q, coenzyme Q or ubiquinone; BN-PAGE, blue native polyacrylamide gel electrophoresis; OXPHOS, oxydative phosphorylation.

0145-479X/04/1000-0471/0 © 2004 Springer Science+Business Media, Inc.

Even if AOX is well conserved throughout species, as shown by primary sequence comparison and by cross-reactivity of protozoan AOX protein with monoclonal antibodies raised against plant (*Sauromatum guttatum*) protein (Jarmuszkiewicz *et al*., 1997), its biochemical regulation depends on its phylogenic origin. On one hand, plant AOX is subjected to regulation by the redox state of the enzyme itself (Umbach and Siedow, 1993) and is stimulated by α-keto acids like pyruvate through the formation of a thiohemiacetal with a conserved cysteine (Umbach and Siedow, 1996; Rhoads *et al.*, 1998). On the other hand, fungal and protozoan AOXs that do not possess this chemically activated cysteine are strongly stimulated by purine 5′-monophosphate nucleotides like GMP and AMP, in pH-dependent way as shown for *A. castellanii* AOX (Jarmuszkiewicz *et al*., 2002a). Plant- and fungi-type AOXs also differ at the level of their molecular organization, as plant oxidase is a functional non-covalent dimer (Umbach and Siedow, 1993) and fungi-type oxidase is a functional monomer (Jarmuszkiewicz *et al*., 1997; 2000). Nevertheless, the engagement of both plant- and fungi-type AOXs in overall respiration is under the control of the redox state of ubiquinone (Q) and it occurs when Q is rather reduced but not necessarily when the cytochrome pathway is kinetically saturated (Moore *et al*., 1988; Jarmuszkiewicz *et al*., 1998a; Sluse and Jarmuszkiewicz, 2000).

Recently, we have observed in *A. castellanii* mitochondria that kinetic behaviour of AOX is influenced by the cytochrome pathway activity and reciprocally: BHAM has an influence on the relationship between the rate of ADP phosphorylation and the Q reduction level, and inhibition of cytochrome *c* oxidase by cyanide has an influence on the relationship between the rate of AOX-sustained O_2 consumption and the Q reduction level (Jarmuszkiewicz *et al*., 2002b). Indeed, at a given Q reduction level, both rates increase in the presence of inhibitor of the other pathway. The observed increase could appear to be obvious as the two pathways share the same oxidizable substrate ubiquinol (QH_2), but not when it occurs at the same Q reduction level where each rate must remain unchanged since the substrate concentration remains the same. This new type of interplay between the cytochrome pathway and AOX, at a given Q reduction level, may be explained either by an indirect functional interaction or by a direct protein–protein interaction between the two pathways, both types of interaction not being mutually exclusive. Considering the indirect functional connection, two complementary hypothesis have been made (Jarmuszkiewicz *et al*., 2002a): (i) activation of the alternative oxidase in the cyanide-inhibited mitochondria at a given Q reduction level could be due to the high sensitivity of AOX to the matricial pH which is lower when the cytochrome pathway proton pumps are inactive, and (ii) activation of the oxidative phosphorylation in BHAM-inhibited mitochondria at a given Q reduction level is due to the decrease in a H^+ leak pathway which is linked to the AOX activity. Considering the direct interaction, it implies an association between AOX and the two cytochrome pathway complexes (one or both) through protein–protein interactions that could depend on conformational changes induced by their ligand-binding sites occupancy and/or by the reduction level of their redox centers.

Thus, it is interesting to determine the protein–protein interactions in native condition where characteristics of mitochondrial membrane proteins are preserved. A powerful technique for identification of direct membrane protein–protein interactions is the blue native-polyacrylamide gel electrophoresis (BN-PAGE) (Schägger, 2001). This technique is used for native preparation and characterization of respiratory chain complexes. It allows molecular weight determination, oligomeric state characterization, detection of subcomplexes and supercomplexes. The subunit composition of the multiprotein complexes can be determined by excision of selected bands that are further identified by SDS-PAGE (resolution in a second dimension) and/or by immunodetection (selective identification of a given protein).

In this study, we have investigated by BN-PAGE the respiratory chain complex pattern of *A. castellanii* mitochondria using the pattern of tomato *L. esculentum* as plant reference. Complexes exhibiting NADH dehydrogenase and cytochrome *c* oxidase activities have been identified by enzymatic staining of the BN polyacrylamide gels. Immunodetection of AOX has been performed after SDS-PAGE of bands excised from the first dimension BN-PAGE gels. Two conditions have been examined: when AOX is abundant, i.e., in ripe tomato mitochondria and in *A. castellanii* mitochondria from exponential phase of growth, and when AOX is scarce, i.e., in green mature tomato mitochondria and in *A. castellanii* mitochondria from stationary phase. In the present work, we show in both *A. castellanii* and tomato mitochondria that AOX protein interacts broadly with respiratory chain complexes when its expression level is high, but that AOX is specifically associated with complex III independently from its concentration.

MATERIAL AND METHODS

A. castellanii Culture and Mitochondria Isolation

Soil amoeba *A. castellanii*, strain Neff, was cultured as described previously (Jarmuszkiewicz *et al*., 1997).

Trophozoites of amoeba were collected after 34 and 78 h following inoculation at the exponential phase (cell density of about 4–5 $\times$ 10^6 cells/mL) and at the stationary phase (cell density of about 10–12 $\times$ 10^6 cells/mL), respectively. Mitochondria were isolated and purified on a self-generating Percoll gradient (31%) as described before (Jarmuszkiewicz *et al*., 1997).

L. esculentum Culture and Mitochondria Isolation

Tomato (*Lycopersicon esculentum* cv Merveilles du marché) plants were cultivated in a green house of the Botanical Institute under 60 PAR (photosynthetic active radiation), 16-h light/8-h dark at 20°C using standard horticultural practices. Fruits were harvested at the green mature and full ripe stages. Mitochondria were isolated after homogenisation by differential centrifugation (Almeida *et al*., 2002). Mitochondria were purified on a self-generating Percoll gradient (Jarmuszkiewicz *et al*., 1998b). Percoll concentration was 21% for mature green fruits and 18% for ripe fruits. Protein concentration was determined by the Biuret method (Gornall *et al*., 1949).

BN-PAGE Electrophoresis

To perform BN-PAGE (Schägger and Von Jagow, 1991; Schägger, 2001). We used a discontinuous system composed by a 5–18% polyacrylamide separating gel and a 4% polyacrylamide stacking gel. Gel buffer contained 25 mM Bis-Tris–HCl, pH 7.0, and 650 mM ε-amino-*n*-caproic acid (ACA). The anode buffer consisted of 25 mM Bis-Tris–HCl, pH 7.0, and the cathode buffer of 50 mM tricine, 15 mM Bis-Tris–HCl and 0.02% Coomassie blue G250, pH 7.0. For sample preparation, mitochondrial suspensions were centrifuged at 15,000 $\times$ g (10 min.) and mitochondrial pellets were suspended in the ACA buffer (40 μL of ACA buffer for 200 μg of mitochondrial protein) containing 0.75 M ACA, 0.5 mM Na_2EDTA, 50mM Bis-Tris–HCl, pH 7.0. Proteins were solubilized by addition of 10% *n*-dodecylmaltoside solution in a protein:detergent ratio of 1:2:5 (w/w). Samples were centrifuged for 20 min at 20,000 $\times$ g and a 5% Blue G250 solution in 750 mM ACA buffer, pH 7.0, was added to the supernatants in a ratio dye:detergent of 1:10 (w/w). Urease (545 and 272 kDa) and BSA (132 and 66 kDa) were used as apparent molecular weight standards. Standards were at a concentration of 5μg/μL in loading buffer consisting of 750 mM ACA, 1% *n*-dodecylmaltoside and 0.5% Coomassie blue G250. Gels were run at 7°C in a PROTEAN® II Xi (BioRad) using a continuous cooling water system. Electrophoresis was performed during 45 min at 7 mA constant and then during 2 h at 15 mA constant. When the blue cathode buffer reached the middle of the separating gel, the cathode buffer was replaced by the same buffer without blue and electrophoresis was carried out overnight at 500 V constant.

Identification of Oxidative Phosphorylation (OXPHOS) Enzymes by Chemical Staining of BN-PAGE Gels

Enzymes with NADH dehydrogenase activities were detected by incubating BN-PAGE gel (protected from light) during 20 min in a 100 mM MOPS-KOH buffer (pH 8.0) containing 1 mg/mL nitroblue tetrazolium (NBT) and 0.2 mM NADH (Grandier-Vazeille and Guérin, 1996).

Enzymes with cytochrome *c* oxidase activity were detected by incubating BN-PAGE gel 20 min in a 10 mM MOPS-KOH buffer (pH 7.4) containing 220 mM sucrose, 2.3 mM diaminobenzidine (DAB), 1 mg/mL cytochrome *c* and 2 μg/mL catalase (Seligman *et al.*, 1968).

Protein patterns were determined by Coomassie blue R-250 coloration of BN-PAGE gel band and apparent molecular weights were estimated by comparison with molecular standards. Gels were fixed in 50% methanol 10% acetic acid solution, discoloured in 10% methanol and 10% acetic acid solution and kept at 4°C in 10% acetic acid solution.

Tricine-SDS-PAGE Electrophoresis

SDS-PAGE (Schägger and Von Jagow, 1987) was performed using a 4% polyacrylamide stacking gel and a 12% polyacrylamide separating gel in PROTEAN® II Xi (BioRad). For second dimension separation, BN-PAGE strips were denaturated by 15 min incubation at 60°C in the BN gel buffer additionally containing 1% SDS and 1% β-mercaptoethanol during 15 min and then in the same solution without β-mercaptoethanol during 15 min. Bands corresponding to complexes were cut off and poured down into wells of the 4% polyacrylamide concentration gel, avoiding bubbles (Kuoen *et al*., 1986). Prestained low molecular weight markers were used (BioRad). Mitochondrial proteins (400 μg), used as positive control for AOX detection, were solubilized in the denaturating sample buffer containing 2% (w/v) SDS, 80 mM Tris–HCl, pH 6.8, 10% (v/v) glycerol, 30 mM dithiothreitol, 0.5% β-mercaptoethanol and 0.025% bromophenol blue. Anode buffer contained 0.2 M Tris–HCl, pH 8.9, and cathode buffer contained 0.1 M tricine, 0.1% SDS and 0.1 M

Tris–HCl, pH 8.25. Gels were run at 8°C, 100 V constant until migrating blue front entered the separating gel, and then 200 V were applied during 5 h.

Western Blotting and Immunodetection of AOX

BN-gel proteins were electrotransfered on PVDF membrane as described by Jänsch *et al.* (1996) and Schägger (2001). Electrotransfer buffer contained: 25 mM Tris–HCl, pH 8.3, 0.192 M glycine, 10% methanol, and 0.05% SDS. A pre-blot was made in order to remove the excess of Coomassie blue (semi-dry transfer at 20 V, 5 min), followed by transfer on a new membrane (20 V constant, 55 min). Second dimension gel proteins were electrotransfered on PVDF membrane (semi-dry transfer at 240 mA, 45 min). Membranes were blocked overnight in 5% skimmed milk blocking solution. Immunodetection of AOX using monoclonal antibodies raised against the *S. guttatum* protein (generously supplied by Dr. T.E. Elthon, University of Nebraska, Lincoln) was carried out following the BM chemiluminescence Western blotting kit (mouse/rabbit) instructions guide (Roche). The AOX bands (approximately 35–36 kDa) were detected by chemiluminescence (Boehringer system).

RESULTS

Identification of OXPHOS Complexes

The pattern of plant respiratory chain complexes and their respective molecular weight has been previously analysed by BN-PAGE (Jänsch *et al.*, 1996). Conversely, very few information is available about *A. castellanii* respiratory chain complex pattern. In order to identify and characterize *A. castellanii* respiratory chain complexes, we used tomato fruit mitochondria as reference. Pattern comparison between each type of mitochondria was therefore achieved by electrophoretic migration on the same BN-PAGE gel. Coomassie blue staining of BN gels showed that the protein band pattern was slightly different for amoeba and tomato mitochondria (Fig. 1) as described latter. Furthermore, amoeba respiratory chain complexes were identified on the basis of their apparent molecular weight when compared to tomato mitochondria complexes and according to specific enzymatic staining of bands corresponding to the NADH dehydrogenase (complex I and NADH dehydrogenases) and cytochrome *c* oxidase (complex IV) activities (Fig. 1). The bands with cytochrome *c* oxidase activities were coloured

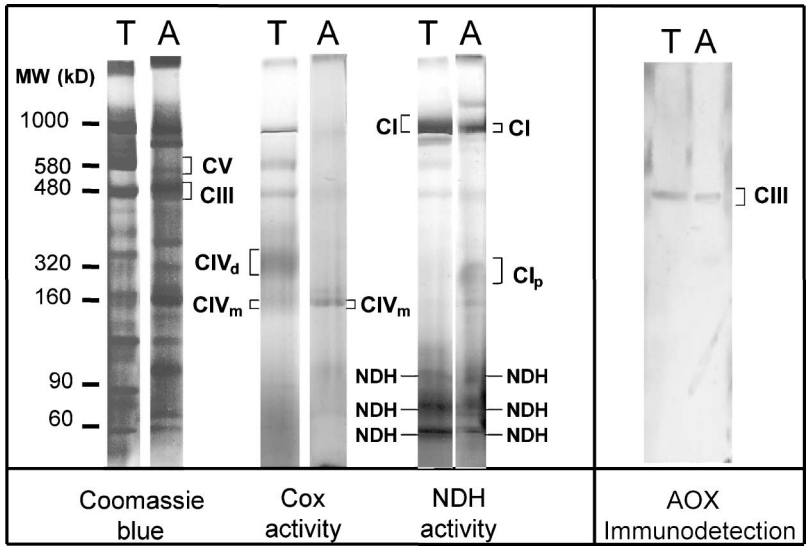

Fig. 1. Blue native gel electrophoresis of mitochondrial protein complexes from tomato and *Acanthamoeba castellanii*. Gels were loaded with 200 μg of total mitochondrial protein of green mature tomato (T) and *A. castellanii* from the stationary phase of growth (A). Coomassie stained gel showed protein pattern of OXPHOS complexes. The complexes were identified according to their molecular weight and to the NADH dehydrogenase (NDH) or cytochrome *c* oxidase (Cox) activities by enzymatic staining. CI, NADH–ubiquinone oxidoreductase (complex I); CIp, peripheral arm of complex I; CIII, ubiquinol–cytochrome *c* oxidoreductase (complex III); CIVm, monomeric form of cytochrome *c*oxidase (complex IV); CIVd, dimeric form of complex IV; NDH, NADH dehydrogenases; CV, ATP synthase. The AOX immunodetection was performed on BN-gel using antibodies raised against AOX protein of *S. guttatum.*

in brown due to the formation of oxidized DAB precipitate. Tomato mitochondria exhibited 160 kDa monomeric and 320 kDa dimeric forms of complex IV, while *A. castellanii* mitochondria only revealed one monomeric form of 160 kDa (Fig. 1). The reduction of nitroblue tetrazolium corresponding to the NADH dehydrogenase activity led to a dark violet staining. In tomato mitochondria, complex I of apparent molecular weight around 1000 kDa was found and three NADH dehydrogenase bands (around 90, 80, and 60 kDa) were additionally identified by the enzymatic reaction staining. An unexpected lighter form of complex I was also observed by enzymatic staining just below the main complex I band. Concerning *A. castellanii* complex I, a discrete stained band was observed at around 1000 kDa as well as a broad one around 280 kDa that could correspond to a part of the peripheral arm of the complex (which is expected to have half of the size of the full complex) bearing the catalytic site. The three bands characteristic of NADH dehydrogenases were conserved in *A. castellanii* mitochondria when compared to tomato mitochondria. Tomato mitochondria complex III was located at around 480 kDa and ATP synthase was found at around 580 kDa, as previously reported in potato and *Arabidopsis thaliana* mitochondria (Jänsch *et al*., 1996). In *A. castellanii*, bands located at the same molecular weight were attributed to these two complexes. BN-gel electroblotting and immunodetection with antibodies raised against AOX protein of *S. guttatum* revealed a presence of AOX located in the band attributed to complex III both in mitochondria of tomato (green mature) and *A. castellanii* (stationary phase of growth).

Tomato Respiratory Complex Subunit Pattern and AOX Immunodetection

We had previously shown that the AOX protein expression markedly varied during tomato fruit development and ripening on the vine (Almeida *et al.*, 2002). Indeed, the AOX protein level was at least threefold higher in ripe fruit compared to green mature fruit. This significant differences in the AOX content is of utmost importance in regard to putative physical interaction between AOX and one or several OXPHOS complexes, likely the less abundant AOX is the more specific the interaction is. In order to verify our earlier proposal, we checked tomato mitochondria isolated at two different developmental stages, i.e., from green mature and fully red ripe fruits.

Thus, the mitochondrial respiratory chain complexes were further analysed by a second dimension separation under denaturing conditions in order to identify associated subunits of each complex. Therefore, after their native separation on BN first dimension gel and identification according to their apparent molecular weight and enzymatic staining (Fig. 2A), the bands of interest were excised, denaturated and run in SDS-PAGE gel. Afterwards, Coomassie blue stained gels exhibited the subunit pattern characteristic of each excised complex (Fig. 2B). In the first lane, the numerous subunits were characteristic of complex I as previously shown in potato (Jänsch *et al*., 1996) but also in bovine heart mitochondria (Schägger *et al*., 1994). The second lane corresponding to a lighter form of complex I (Fig. 1) contained the subunits of complex I peripheral arm since the band excised from the BN gel exhibited a dark violet staining characteristic of NADH oxido-reductase activity, and since some subunits of complex I (around 55 kDa and between 35 and 29 kDa) were observed. The third lane corresponded to the ATP synthase according to the apparent molecular weight of the excised band and to the subunits pattern with an intense band at around 55 kDa (Jänsch *et al*., 1996). The fourth lane contained the excised band with the apparent molecular weight of complex III and exhibited the typical doublet (Jänsch *et al*., 1996). The fifth lane contained an excised band of roughly 400 kDa detected in the first dimension gel but without any enzymatic staining. Since a subunit was found around 70 kDa in the second dimension gel, we assumed that this band could correspond to the peripheral arm of complex I that had lost its catalytic subunits (FMN, Fe–S binding N-3). Sixth and seventh lanes corresponded to the monomeric and dimeric form of complex IV according the molecular weight and the brown chemical staining of excised bands. Eighth to tenth lanes were attributed to NADH dehydrogenases as identified by enzymatic staining and molecular weight.

Immunodetection of AOX protein was performed using green mature and red tomato total mitochondrial protein samples as positive control (Fig. 2C). As expected, the intensity of cross-reactivity with AOX antibodies was more pronounced with red fruit mitochondria than with green mature fruit (Almeida *et al*., 2002). Concerning AOX detection within second dimension lanes in green mature mitochondria, a strong reaction was observed in the fourth lane corresponding to complex III (Fig. 2C, green tomato). On the contrary, in red ripe tomato mitochondria, the cross-reactivity with AOX antibodies was observed within lanes evidenced as complex I peripheral arm with and without NADH dehydrogenase activity, complex III, ATP synthase and monomeric/dimeric complex IV but not within lanes corresponding to NADH dehydrogenases (Fig. 2C, red tomato). Therefore, the cross-reactivity with AOX antibodies in lanes issued

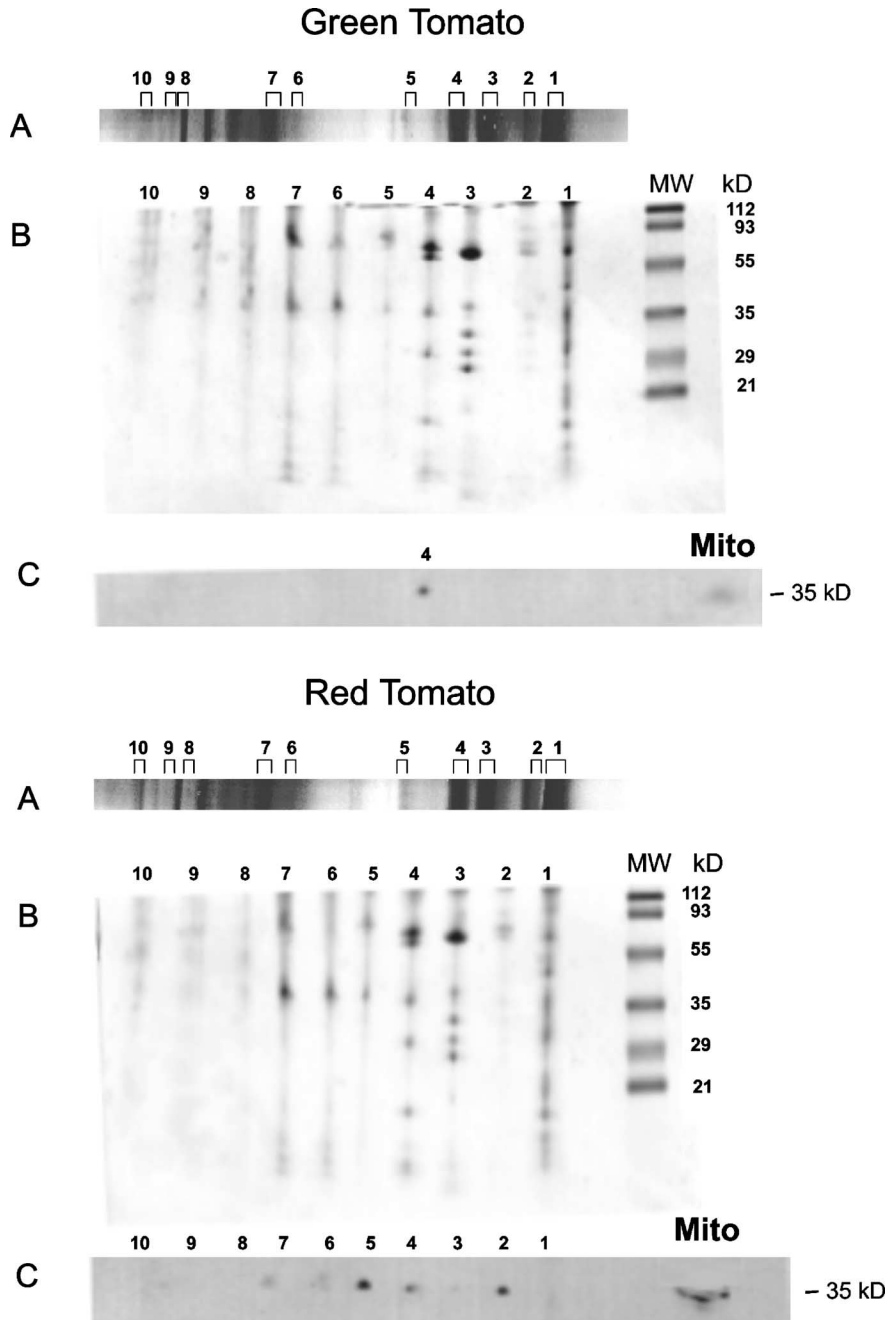

Fig. 2. OXPHOS complexes resolved by two-dimension followed by AOX immunodetection of mitochondria of green mature and red ripe on the vine tomato. (A) BN-PAGE first dimension gel strips loaded with 400 μg of total mitochondrial proteins. The numbers above the strips indicate the band that was excised to perform the second dimension. (B) SDS-PAGE second dimension gels show the subunit pattern of the selected bands. MW, pre-stained low molecular weight markers (BioRad). (C) Photographic films show AOX immunodetection by chemiluminescence within second dimension wells. Total mitochondrial protein (400 μg) samples were used as positive control. 1, complex I; 2, complex I peripheral arm; 3, ATP synthase; 4, complex III; 5, lighter form of complex I peripheral arm (without catalytic center); 6, dimeric form of complex IV; 7, monomeric form of complex IV; 8–10, NADH dehydrogenases.

from high molecular weight bands reflected an apparent association of AOX with OXPHOS complexes in native condition. The difference in the apparent association of AOX with OXPHOS complexes observed in tomato mitochondria isolated at two distinct physiological states seems to be linked to the amount of expressed AOX.

A. castellanii Respiratory Complex Subunit Pattern and AOX Immunodetection

In *A. castellanii* mitochondria, the amount of immunologically detectable AOX protein varied depending on the cell culture stage (Jarmuszkiewicz *et al*., 1997). The highest level of AOX protein was observed in the exponential phase of growth (around 30 h after inoculation) and the lowest in the late stationary phase (around 72 h after inoculation) where AOX content dropped 10-fold (Jarmuszkiewicz *et al*., 1997). To investigate whether physical interaction between AOX and OXPHOS complexes was influenced by protein amount that varied according to the age of *A. castellanii* cell culture, mitochondria isolated from 34 and 72 h cell cultures were subjected to BN-PAGE followed by SDS-PAGE and immunodetection (Fig. 3). Respiratory chain complexes resolved in BN-PAGE were first identified according to their apparent molecular weight and chemical staining when possible (Fig. 3A). Afterwards, Coomassie blue staining of SDS-PAGE gels showed subunits of each band excised (Fig. 3B). The first lane corresponded to complex I as revealed by first dimension colorimetric assay. The second lane corresponded to ATP synthase according to the apparent molecular weight and the presence of a characteristic band of 55 kDa. The third lane contained the excised band with apparent molecular weight of complex III. The fourth to sixth lanes could correspond to different forms of the hydrophobic part of complex I as no staining was observed in BN gel and as three bands of around 50–55, 40 and 35 kDa were observed in each lane and could correspond to the plant nad 5 (quinone binding), nad 4, and nad 2 (unknown function), respectively (Rasmusson *et al.,* 1998). It seems that the smaller is the hydrophobic part of complex I the more abundant it is (Fig. 3, lanes 4–6). The seventh lane corresponded to the monomeric form of complex IV as revealed by chemical staining and an apparent molecular weight in the first dimension lane (160 kDa). The eighth lane was violet stained, indicating a NADH oxidoreductase activity. Its apparent molecular weight was below that of complex IV monomeric one (compared to Fig. 1) indicating that it could correspond to a small part of the peripheral arm of complex I that has kept its catalytic site but has lost labile subunits compared to the peripheral arm of complex I identified in Fig. 1. The last three lanes corresponded to the NADH dehydrogenases because of violet staining and adequate molecular weights.

Immunodetection of AOX protein was performed using total mitochondrial proteins samples as positive control (Fig. 3C). As expected, the cross-reactivity with AOX antibodies was more intense for mitochondria isolated from *A. castellanii* in exponential phase of growth (34 h cell culture) compared to stationary phase (78 h cell culture). For *A. castellanii* mitochondria from the exponential phase of growth (the high level of AOX), all complexes (complex I and all its partial forms, ATP synthase, complex III and monomeric complex IV) exhibited immunoreactivity except for the three low molecular weight NADH dehydrogenases (Fig. 3C, amoeba 34 h). On the contrary, in mitochondria from amoeba at the stationary phase of growth (very low content in AOX), the AOX protein was only detected in the third lane corresponding to complex III (Fig. 3C, amoeba 72 h). As already observed with tomato mitochondria, the difference of apparent AOX association with respiratory chain complexes according to the phase of amoeba cell culture growth could be attributed to the relative amount of AOX.

DISCUSSION

We have previously shown that the steady-state activity of the two quinol oxidizing pathways of *A. castellanii* mitochondria (cytochrome pathway and AOX) increases with the Q reduction level (up to 80%) independently of the reducing substrate (succinate or external NADH) (Jarmuszkiewicz *et al.*, 2002b). This indicates that the active Q pool is homogenous (no micro-compartmentation in the membrane) and that AOX has no direct interaction with the external NADH dehydrogenase. This conclusion is supported by the present work (Fig. 3C, lanes 9–11). However, it has been observed that both quinol oxidizing pathways do not work independently leading to an interplay that could be only explained either by indirect functional connections or by direct protein–protein interactions (not mutually exclusive). Recently, we have also shown that the stimulation of *A. castellanii* AOX by GMP is strongly pH dependent, likely implicating protonation/deprotonation process at the level of ligand and protein with an optimum pH of 6.8 (Jarmuszkiewicz *et al.*, 2002a). Moreover, Q redox state and pH collaborate to set the AOX activity. This pH sensitivity of AOX could partly explain (see Introduction) the indirect functional interaction supporting the interplay between cytochrome pathway and AOX. Notwithstanding this functional

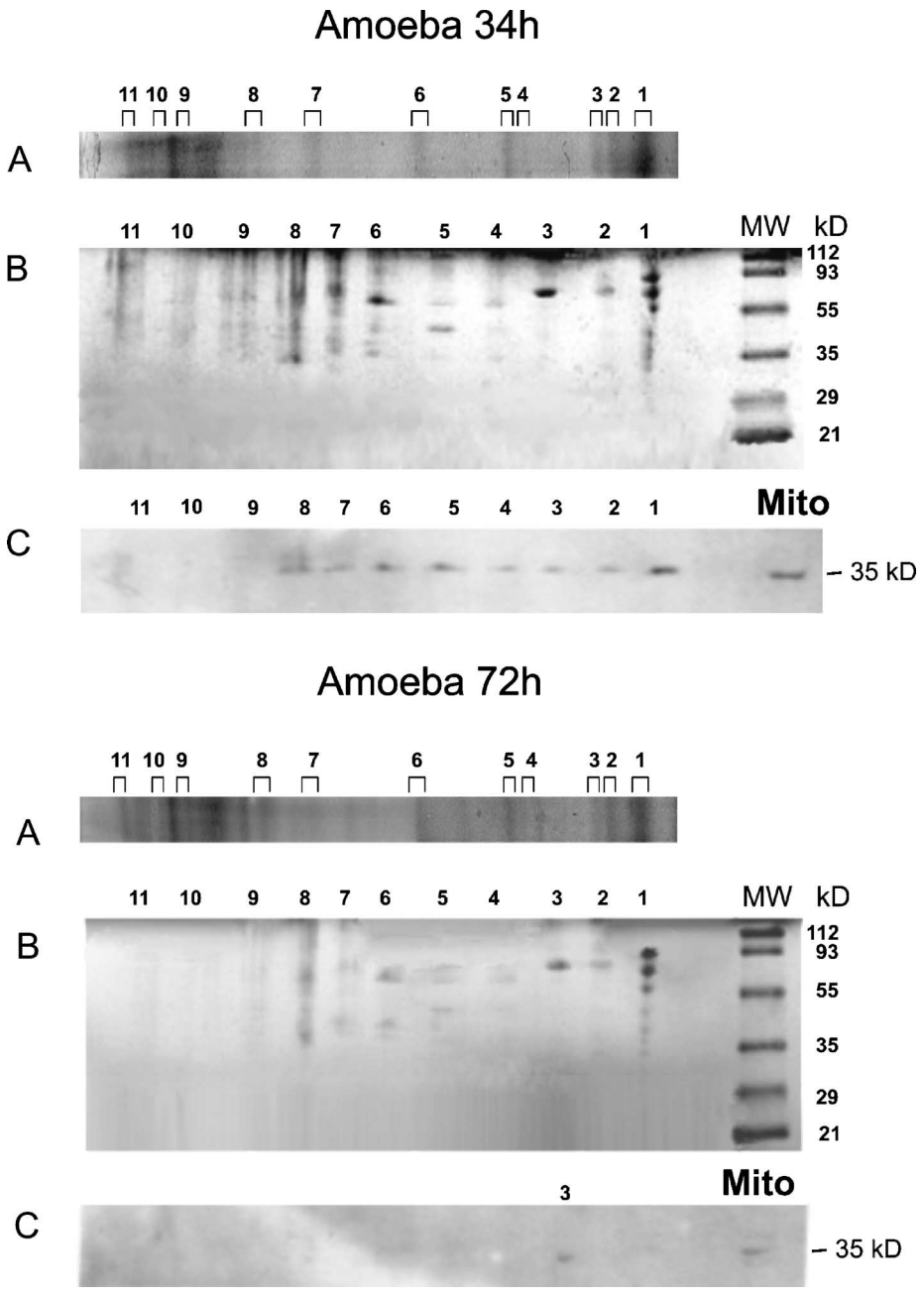

Fig. 3. OXPHOS complexes resolved by two-dimension followed by AOX immunodetection of mitochondria of *A. castellanii* from exponential growing phase and stationary phase. (A) BN-PAGE first dimension gels strips loaded with 400 μg of total mitochondrial proteins. The numbers above the strips indicate the band that were excised to perform the second dimension. (B) SDS-PAGE second dimension gels show the subunits pattern of the selected bands. MW, pre-stained low molecular weight markers (BioRad). (C) Photographic films show AOX immunodetection by chemiluminescence within second dimension wells. Total mitochondrial protein (400 μg) samples were used as positive control. 1, complex I; 2, ATP synthase; 3, complex III; 4 to 6, hydrophobic part of complex I; 7, monomeric form of complex IV; 8, peripheral arm of complex I; 9–11, NADH dehydrogenases.

interplay, this work provides the first evidence of direct protein–protein interactions between quinol oxidizing pathways. An unexpected observation is the apparent association of plant and protozoan AOX with OXPHOS complexes depending on the oxidase expression level. A "specific" interaction is detected with complex III when AOX expression is low contrarily to the "stochastic" interactions observed with all large OXPHOS complexes when AOX is abundant. The latter non-selective interactions could be artefacts as it could be explained by the fact that detergent micelles of large multiprotein complexes can "engulf" small proteins like AOX if they are close enough. This could lead to cross-reactivity of antibodies with every OXPHOS complexes during immunodetection. A possible explanation of this phenomenon could be the existence of supercomplexes (I, III, IV) (Schägger and Pfeiffer, 2000, 2001; Schägger, 2002) in equilibrium with the free complexes according to physiological conditions (Lenaz, 2001) that could contain AOX molecules.

According to our previous observations with mitochondria isolated from *A. castellanii* in exponential phase of cell culture growth (high AOX expression level), the heterologous complex III–AOX association exhibits the increase in AOX activity when cyanide is present (Jarmuszkiewicz *et al*., 2002b). It can be hypothesized that the presence of cyanide reduces the complex III redox centres, inducing conformational changes sensed by the tightly associated AOX through protein–protein interactions that consequently activate AOX. This hypothetical mechanism could occur in vivo when phosphate potential increases and electron flux decreases concomitantly in the cytochrome pathway, and could allow consumption of the excess of reducing power by AOX through complex III–AOX interaction. The reciprocal effect could be also assumed, i.e., complex III is activated when AOX activity is inhibited by BHAM. Then in vivo, when the AOX activity decreases because of a decrease in the reduction state of Q, the complex III activity would increase in order to promote the use of reducing power by the cytochrome pathway for ATP production.

We can conclude that the evidenced physical interaction between AOX and complex III in *A. castellanii* as well as in tomato fruit mitochondria could not only explain partly the kinetical interplay between the two quinol oxidizing pathways observed in amoeba, but also could suggests that such a kinetic interplay exists in plant mitochondria. Moreover, the physical interaction between complex III and AOX seems to be universal as it is observed both for the fungi-type AOX and for the plant-type AOX, independently of the monomeric or dimeric status of the enzyme and of its activation by purine nucleotides (fungi type) or α-keto acids (plant type).

ACKNOWLEDGMENTS

This work was supported by grants from Belgian FRFC (no. 2.4517.00) and accord communauté Wallonie-Bruxelles/Pologne. R. N and P. D received Belgian F.R.I.A Ph.D. fellowships.

REFERENCES

Almeida, A. M., Navet, R., Jarmuszkiewicz, W., Vercesi, A. E., Sluse-Goffart, C. M., and Sluse, F. E. (2002). *J. Bioenerg. Biomembr.* **34**, 487-498.

Gornall, A. G., Bradawill, C. J., and David M. M. (1949). *J. Biol. Chem.* **177**, 751–766.

Grandier-Vazeille, X., and Guérin, M. (1996). *Anal. Biochem.* **242**, 248–254

Jänsch, L., Kruft, V., Schmitz, U. K., and Braun, H. P. (1996). *Plant J.* **9**, 357–368.

Jarmuszkiewicz, W., Wagner, A. M., Wagner, J. M., and Hryniewicka, L. (1997). *FEBS Lett.* **411**, 110–114.

Jarmuszkiewicz, W., Sluse-Goffart, C. M., Hryniewiecka, L., Michejda, J., and Sluse F. E. (1998a). *J. Biol. Chem*. **273**, 10174–10180.

Jarmuszkiewicz, W., Almeida, A. M., Sluse-Goffart, C. M., Sluse, F. E., and Vercesi, A. E. (1998b). *J. Biol. Chem*. **273**, 34882–34886.

Jarmuszkiewicz, W., Milani, G., Fortes, F., Schreiber, A. Z., Sluse, F. E., and Vercesi, A. E., (2000). *FEBS Lett*. **467**, 145–149.

Jarmuszkiewicz, W., Hryniewiecka, L., and Sluse, F. E. (2002a). *J. Biomembr. Bioenerg*. **34**, 221–226.

Jarmuszkiewicz, W., Sluse F. E., Hryniewiecka, L., and Sluse-Goffart, C. M. (2002b). *J. Biomembr. Bioenerg*. **34**, 31–40.

Kuoen, D. R., Roberts, P. J., and Cottingham, I. R. (1986). *Anal. Biochem*. **153**, 221–226.

Lenaz, G. (2001). *FEBS Lett*. **509**, 151–155.

Moore, A. L., Dry, I. B., and Wiskich, J. T. (1988). *FEBS Lett*. **235**, 76–80.

Rasmusson, A. G., Heiser, V., Zabaleta, E., Brennicke, A., and Grohmann L. (1998). *Biochim. Biophys. Acta* **1364**, 101–111.

Rhoads, D. M., Umbach, A. L., Sweet, C. R., Lennon, A. M., Rauch G. S., and Siedow, J. N. (1998). *J. Biol. Chem*. **273**, 30750–30756.

Schägger, H., and Von Jagow, G. (1987). *Anal. Biochem.* **166**, 368–379.

Schägger, H., and Von Jagow, G. (1991). *Anal. Biochem*. **199**, 223–231.

Schägger, H., Cramer, W. A., and Von Jagow, G. (1994). *Anal. Biochem*. **217**, 220–230.

Schägger, H., and Pfeiffer, K. (2000). *EMBO J.* **19**, 1777–1783.

Schägger, H. (2001). *Meth. Cell. Biol*. **45**, 231–244.

Schägger, H., and Pfeiffer K. (2001). *J. Biol. Chem*. **276**, 37861–37867.

Schägger, H. (2002). *Biochim. Biophys. Acta* **1555**, 154–159.

Seligman, A. M., Karnovsky, M. J., Wasserkrug, H. L., and Hanker, J. S. (1968). *J. Cell. Biol.* **38**, 1–3.

Sluse, F. E., and Jarmuszkiewicz, W. (2000). *Braz. J. Med. Biol. Res*. **33**, 259–268.

Umbach, A. L., and Siedow, J. N. (1993). *Plant Physiol*. **103**, 845–854.

Umbach, A. L., and Siedow, J. N. (1996). *J. Biol. Chem*. **271**, 25019–25026.